Tethered UAV-based Communications for Under-connected Near-shore Maritime Areas

Sahar Ammar, Osama Amin, Basem Shihada
Computer, Electrical and Mathematical Science and Engineering Division,
King Abdullah University of Science and Technology (KAUST),
Thuwal, Saudi Arabia
E-mail: {sahar.ammar, osama.amin, basem.shihada}@kaust.edu.sa

***Abstract*—Maritime activities, including fisheries, maritime transportation, and surveillance, are expected to transfer multimedia data to remote users, which requires the establishment of reliable backhaul communication links from the marine vessels to the core network. Tethered Unmanned Aerial Vehicles (UAVs), which are connected to a sufficient power source and high-data-rate optical fiber, can be adopted in near-shore maritime communications for coverage extension. In this paper, we investigate the use of tethered UAVs in three scenarios, where the UAV can be either installed on the shore, tethered to the ship, or both. To study the coverage performance, we examine the outage probability in each scenario for both uplink and downlink, and we optimize it to derive the optimal UAV placement. Although the optimization problem, in terms of the UAV tether length and the angle it makes with the horizontal, is non-convex, we formulate and solve a simplified problem where the outage probability is minimized with respect to the channel gain to obtain the optimal UAV position. The simulation results show that using two UAVs, one onshore and one on the ship, provides more reliable connectivity on the uplink and downlink compared to the other two scenarios.**

***Index Terms*—Maritime Communications, Tethered UAVs, Placement Optimization.**

I. Introduction

Maritime activities have expanded over the last few decades to include fisheries and aquaculture, maritime transportation, and marine life monitoring. Such activities require reliable maritime communications in order to transfer multimedia data to remote users over the network [1]. Thus, there is a need for robust backhaul links connecting the ships to the core network. Nonetheless, while underwater communications have gained a lot of attention recently [2]–[5], establishing maritime communication links to connect marine vessels to the core network remains a challenge that requires further research. This is due to the low user density, the vast ocean areas that should be covered, and the difficulty of deploying typical base stations in the open seas [6]. Conventional maritime communication technologies are based on on-shore base stations providing basic services including automatic identification systems (AIS), text messaging and voice calling. To support broadband connectivity, the authors of [7] proposed a maritime communication system based on the Long-Term Evolution (LTE) technology. Through a test-bed composed of several ships and base stations installed along the coastline, they achieved a few Mbps data rate over 100 km link range. Meanwhile, efforts have been dedicated to enable connectivity in such remote under-connected areas, using integrated terrestrial and non-terrestrial networks [8], [9]. Specifically, researchers have developed satellite-based maritime communication systems, to expand the coverage area. In particular, Inmarsat Global Xpress is a series of satellite communication systems, composed of Geostationary Earth Orbit (GEO) satellite constellations [10]. They offer global data services over the Ka-band with a data rate of 50 Mbps on downlink and a few Mbps on uplink.

Nonetheless, satellite-based communications not only suffer from large propagation distances and restricted on-board resources leading to significant delays and limited data rates but also require international regulations can pose political complications [6], [11]. Moreover, unlike cargo and cruise ships, maritime users particularly in fishing villages and small islands cannot afford the use of satellite-based systems. This is due to their high costs and large antennas which cannot be installed on fishing and small boats. Consequently, there is an increasing need for connectivity solutions that are suitable for this type of vessel, especially with the growing economy in the fisheries and aquaculture industry. Statistics reveal that the estimated growth of the global seafood market is expected to increase from around 237 billion USD in 2023 to approximately 331 billion USD by 2028 [12]. Therefore, researchers are dedicating their efforts to develop communication systems based on UAVs, providing promising alternatives to extend the terrestrial network. The UAVs can expand the near-shore coverage, by acting as relaying units to connect marine vessels and on-land base stations. Because of their cost-efficient, simple and flexible deployment, these aerial platforms are suitable for maritime communications. In [11], UAVs are used in a hybrid satellite-terrestrial network for coverage improvement in broadband on-demand maritime communications. However, UAVs are battery-dependent which limits their flight time, and affects the link reliability. Tethered UAVs can alleviate such an issue, at the cost of restricted mobility and limited coverage compared to untethered UAVs [13]. The tether linking the UAV to an anchor unit, connecting it to a power supply. It also incorporates a connectivity wire which can be a copper cable or an optical fiber, enabling high data rates.

Few studies have been reported in the literature developing tethered UAV-based maritime communications. The BLUECOM+ project [14] presents a cost-effective broadband

communication solution. Using helikites tethered to on-land and ocean platforms, they achieve 3 Mbps over 100 km of two-hop communication link. In [15], [16], the authors employed tethered UAVs connected to edge servers on the coastline in a hybrid satellite UAV terrestrial network for on-demand maritime coverage. In [15], they optimize the rate of users served by Terrestrial Base Stations (TBSs) and UAVs while ensuring a minimum interference with satellite users. In [16], they adopt Non-Orthogonal Multiple Access (NOMA) technique to serve the sparsely distributed users. Also, they propose a joint power allocation scheme that maximizes the network sum rate taking into account the interference between the network's segments and guaranteeing a minimal quality-of-service requirement.

In this paper, we focus on the use of tethered UAVs in maritime communications aiming to connect users aboard marine vessels to the core network. While none of the aforementioned works study the case where UAVs are tethered to the ships, we not only investigate this scenario but also the cases where the UAVs are installed on the shore, or on both sides. Particularly, we investigate the coverage performance for the three scenarios and we derive the optimal placement of the UAV in each case while minimizing the outage probability. We also compare the coverage performance of the three links for both uplink and downlink. To the best of our knowledge, this is the first work that considers the use of UAVs tethered to marine vessels in maritime communications. The rest of the paper is organized as follows, Section II describes the system model particularly the channel modeling of each scenario. Section III deals with the optimization of the outage probability and the derivation of the UAVs optimal placement. Section IV discusses the numerical results, followed by the paper conclusion in Section V.

II. System Model

We consider three scenarios of tethered UAV-based maritime communications, as shown in Fig.1. First, we assume that the UAV (sUAV) is tethered to the ship at sea, providing connectivity through a wireless link TBS$-$sUAV with the TBS on land. Second, we consider the case where the tethered UAV (gUAV) is installed on the ground and connected to the marine vessel through another wireless link Ship$-$gUAV, which is similar to the scenario in [16]. Third, we adopt two UAVs on both sides creating an Air-to-Air link gUAV$-$sUAV.

To simplify the analysis, for each link $k = 1, 2, 3$, we use a 2D coordinate system (x_k, y_k) modeling the positions of the different components in each scenario, as illustrated in Fig.1. The coordinates of the TBS, antenna ship, and the two UAVs are as follows:

- Link 1 (TBS$-$sUAV): $\begin{cases} C^{\text{TBS}}_{(x_1,y_1)} = (x_{\text{TBS}}, y_{\text{TBS}}) \\ C^{\text{sUAV}}_{(x_1,y_1)} = (x_1, y_1) \end{cases}$
- Link 2 (Ship$-$gUAV): $\begin{cases} C^{\text{AntS}}_{(x_2,y_2)} = (x_{\text{AntS}}, y_{\text{AntS}}) \\ C^{\text{gUAV}}_{(x_2,y_2)} = (x_2, y_2) \end{cases}$
- Link 3 (gUAV$-$sUAV): $\begin{cases} C^{\text{sUAV}}_{(x_3,y_3)} = (x_3^{\text{sUAV}}, y_3^{\text{sUAV}}) \\ C^{\text{gUAV}}_{(x_3,y_3)} = (x_3^{\text{gUAV}}, y_3^{\text{gUAV}}) \end{cases}$

The coordinates of the sUAV and gUAV can be written in terms of the UAV tether length and the angle it makes with the $x-$axis as follows:

- For sUAV:

$$\begin{cases} x_1 = \eta_1 \cos\theta_1, \\ y_1 = \eta_1 \sin\theta_1, \end{cases}, \begin{cases} x_3^{\text{sUAV}} = x_S - \eta_1 \cos\theta_1, \\ y_3^{\text{sUAV}} = \eta_1 \sin\theta_1, \end{cases}, \tag{1}$$

- For gUAV:

$$\begin{cases} x_2 = \eta_2 \cos\theta_2, \\ y_2 = \eta_2 \sin\theta_2, \end{cases}, \begin{cases} x_3^{\text{gUAV}} = \eta_2 \cos\theta_2, \\ y_3^{\text{gUAV}} = \eta_2 \sin\theta_2, \end{cases}, \tag{2}$$

where η_n, θ_n for $n = 1, 2$ are the tether length and angle of the sUAV and the gUAV, respectively, indicating the placement of the tethered UAVs. Also, x_S denotes the x coordinate of the ship in Link 3.

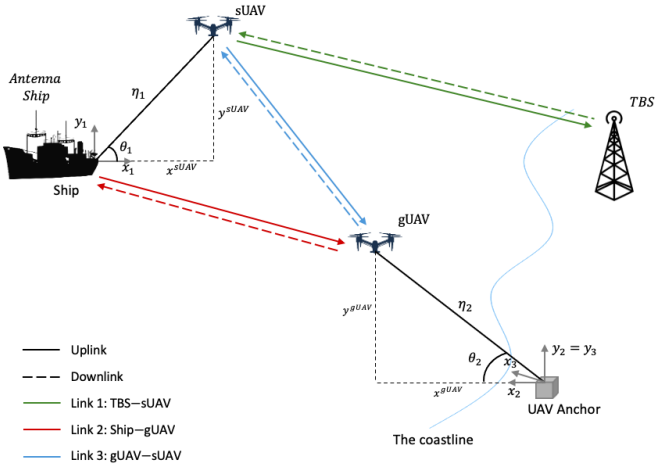

Fig. 1: Illustration of the Tethered UAV-based Maritime Communication.

We examine the performance of the three links for both uplink and downlink scenarios. Three types of wireless channels can be distinguished:

- Air-to-Ground/Sea (AG) channel in the case of the uplink of link 1 and the downlink of link 2.
- Ground/Sea-to-Air (GA) channel in the case of the downlink and uplink of link 1 and 2, respectively.
- Air-to-Air (AA) channel, inter-UAV communication in case of the third link for both uplink and downlink.

The modeling of each channel includes the large-scale fading characterized by the path loss of the dominant Line-of-Sight (LOS) component, and the small-scale fading modeled as a Rician fading [17], [18].

A. Large-scale Fading

Assuming the earth's flatness for the considered communication ranges, the path loss of the Air-to-Ground channel can be modeled as follows [11], [17], [18],

$$L_{AG}(d_k)|_{dB} = L_{AG}(d_k^0)|_{dB} + 10\alpha_{AG}\log_{10}\left(\frac{d_k}{d_k^0}\right) + \chi \tag{3}$$

where d_k represents the communication distance, d_k^0 is the reference distance, α_{AG} denotes the path loss exponent and χ

is a zero-mean Gaussian random variable with variance $\sigma\chi$, describing the difference between the measured data and the model in [18].

Moreover, the large-scale in case of the Ground-to-Air and the Air-to-Air channels can be expressed using the Free-space path loss model, as follows [19], [20],

$$L_s(d_k)|_{dB} = 10\alpha_s \log_{10}\left(\frac{4\pi f d_k}{c}\right), \quad s = \{AA, GA\} \quad (4)$$

where α_s denotes the path loss exponent, f and c are the frequency and the light velocity. The link range d_k is expressed in terms of the coordinates of the link components, as

$$d_k = \begin{cases} \sqrt{(x_1 - x_{\mathrm{TBS}})^2 + (y_1 - y_{\mathrm{TBS}})^2}, & k = 1 \\ \sqrt{(x_2 - x_{\mathrm{AntS}})^2 + (y_2 - y_{\mathrm{AntS}})^2}, & k = 2 \\ \sqrt{(x_3^{\mathrm{sUAV}} - x_3^{\mathrm{gUAV}})^2 + (y_3^{\mathrm{sUAV}} - y_3^{\mathrm{gUAV}})^2}, & k = 3 \end{cases}, \quad (5)$$

We note that the distance d_k can also be expressed in terms of the tether length η and the angle θ of the UAV using (1) and (2). Thus, the path loss characterizing the large-scale fading of the uplink (U) and downlink (D) for the k^{th} link is,

$$L_{k,l}(d_k) = \begin{cases} L_{AG}(d_k)|_{dB} & (k,l) = \{(1,U),(2,D)\} \\ L_{GA}(d_k)|_{dB} & (k,l) = \{(1,D),(2,U)\} \\ L_{AA}(d_k)|_{dB} & (k,l) = \{(3,D),(3,U)\} \end{cases}. \quad (6)$$

Thus, the corresponding channel gain can be expressed as,

$$h_{k,l}(d_k) = 10^{-L_{k,l}(d_k)/10}. \quad (7)$$

B. Small-scale Fading

To capture the characteristics of the maritime channel, the small-scale channel fading caused by the weak paths resulting from the multiple sea surface reflections, especially in rough sea situations, is modeled as Rician fading [17]. It is defined by the following distribution,

$$f_{\xi_{k,l}}(x) = \frac{x}{\sigma_{k,l}^2} \exp\left(\frac{-\left(x^2 + \nu_{k,l}^2\right)}{2\sigma_{k,l}^2}\right) I_0\left(\frac{x\nu_{k,l}}{\sigma_{k,l}^2}\right), \quad x \geq 0 \quad (8)$$

where $2\sigma_{k,l}^2$ and $\nu_{k,l}^2$ are the average received power of the multipath components and the LOS component, respectively, and $I_0(.)$ is the first kind of modified Bessel function of the 0^{th} order given by,

$$I_0(x) = \sum_{m=0}^{\infty} \frac{1}{(m!)^2}\left(\frac{x}{2}\right)^{2m}. \quad (9)$$

III. Optimization of tethered UAV location

In this section, we derive the expression of the outage probability, formulate the optimization problem, and solve it to obtain the optimal placement of the tethered UAVs in each scenario.

A. Outage Probability

To investigate the coverage performance of both the uplink and downlink for each scenario, we study the outage probability which is defined as follows,

$$P_{k,l}^{\mathrm{out}} = Pr[\gamma_{k,l} \leq \gamma_{k,l}^{min}], \quad (10)$$

where $\gamma_{k,l}$ is the signal-to-noise ratio (SNR) and $\gamma_{k,l}^{min}$ denotes the minimum SNR value guaranteeing minimal link quality. The SNR is given by

$$\gamma_{k,l} = \frac{P_{k,l} G_{k,l} h_{k,l} \xi_k^2}{\sigma_{N_k}^2}, \quad (11)$$

where $G_{k,l} = G_{k,l}^T G_{k,l}^R$, $G_{k,l}^T$ and $G_{k,l}^R$ are the transmitter and receiver antenna gains, $\sigma_{N_k}^2$ is the Gaussian noise power and $P_{k,l}$ is the transmit power, given by

$$P_{k,l} = \begin{cases} P_{\mathrm{sUAV}}, & (k,l) = \{(1,U),(3,U)\} \\ P_{\mathrm{gUAV}}, & (k,l) = \{(2,D),(3,D)\} \\ P_{\mathrm{TBS}}, & (k,l) = (1,D) \\ P_{\mathrm{AntS}}, & (k,l) = (2,U) \end{cases}. \quad (12)$$

Assuming that $\sigma_{k,l} = 1$, the outage probability can be written in terms of the cumulative distribution function (CDF) of a noncentral chi-squared distribution with two degrees of freedom and noncentrality parameter $\nu_{k,l}^2$,

$$P_{k,l}^{\mathrm{out}} = 1 - Q_1(\nu_{k,l}, \delta_{k,l}), \quad (13)$$

where $\nu_{k,l} = \sqrt{P_{k,l} G_{k,l} h_{k,l}}$, $\delta_{k,l} = \sqrt{\frac{\sigma_{N_k}^2}{P_{k,l} G_{k,l} h_{k,l}} \gamma_{k,l}^{min}}$, and $Q_1(a,b)$ is the Marcum Q-function of first order given by,

$$Q_1(a,b) = \int_b^{\infty} x \exp\left(-\frac{x^2 + a^2}{2}\right) I_0(ax) dx. \quad (14)$$

B. Optimal UAV placement

1) Optimal UAV placement for Link 1 and Link 2:
To maximise the link coverage in each scenario, we minimize the outage probability by finding the optimal placement of the tethered UAV in the 2D plane. Since, the UAV position can be determined by its tether length and its angle with the $x-$axis, the optimization problem ($\mathbf{P_{k,l}}$), $k = 1, 2$ and $l = U, D$, for the first and second links can be written as,

$$(\mathbf{P_{k,l}}): \min_{\eta_k, \theta_k} \quad P_{k,l}^{\mathrm{out}}(\eta_k, \theta_k) \quad (15a)$$

$$\text{s. t.} \quad \eta_{k,min} \leq \eta_k \leq \eta_{k,max}, \quad (15b)$$

$$\theta_{k,min} \leq \theta_k \leq \theta_{k,max} \quad (15c)$$

where $\eta_{k,min}$, $\eta_{k,max}$, $\theta_{k,min}$ and $\theta_{k,max}$ are the minimum and maximum values of the tether length and angle of the sUAV and the gUAV, when $k = 1$ and $k = 2$ respectively.

The outage probability $P_{k,l}^{\mathrm{out}}(\eta_k, \theta_k)$ is expressed, in (13), in terms of the Marcum Q-function with two variables $\nu_{k,l}$ and $\delta_{k,l}$, which are two-variable functions of η_k and θ_k. Thus, the objective function of ($\mathbf{P_{k,l}}$) is a two-variable composition of three functions, which makes the optimization problem not only non-convex, but also, difficult to solve in terms of two variables. Hence, to simplify the problem, we change the variables of the objective function, such that it can be written in terms of one variable which is the channel gain $h_{k,l}$, and the outage probability becomes,

$$P_{k,l}^{\mathrm{out}}(h_{k,l}) = 1 - Q_1\left(A_{k,l}\sqrt{h_{k,l}}, \frac{B_{k,l}}{\sqrt{h_{k,l}}}\right) \quad (16)$$

where $A_{k,l} = \sqrt{P_{k,l}G_{k,l}}$ and $B_{k,l} = \sqrt{\frac{\sigma_{N_k}^2}{P_{k,l}G_{k,l}}\gamma_{k,l}^{min}}$ are constants depending on the system parameters. Then, the simplified optimization problem is,

$$(\mathbf{P'_{k,l}}): \min_{h_{k,l}} \quad P_{k,l}^{\text{out}}\left(h_{k,l}\right) \tag{17a}$$

$$\text{s. t.} \quad H_{k,l,min} \leq h_{k,l} \leq H_{k,l,max}, \tag{17b}$$

where $H_{k,l,min}$ and $H_{k,l,max}$ are the minimum and maximum values of the channel gain. Then, to solve the simplified problem $(\mathbf{P'_{k,l}})$, we examine the objective function in (16), which can be written in terms of a composition of a multivariable function as,

$$P_{k,l}^{\text{out}}\left(h_{k,l}\right) = 1 - Q_1\left(f(h_{k,l}), g(h_{k,l})\right) \tag{18}$$

where $f(h_{k,l}) = A_{k,l}\sqrt{h_{k,l}}$ and $g(h_{k,l}) = \frac{B_{k,l}}{\sqrt{h_{k,l}}}$. The derivative of (18) can be obtained using the multivariable chain rules as follows,

$$\begin{aligned}\frac{\partial P_{k,l}^{\text{out}}(h_{k,l})}{\partial h_{k,l}} = &- \frac{\partial Q_1\left(f(h_{k,l}), g(h_{k,l})\right)}{\partial f(h_{k,l})}\frac{\partial f(h_{k,l})}{\partial h_{k,l}} \\ &- \frac{\partial Q_1\left(f(h_{k,l}), g(h_{k,l})\right)}{\partial g(h_{k,l})}\frac{\partial g(h_{k,l})}{\partial h_{k,l}}\end{aligned} \tag{19}$$

where the partial derivatives of $Q_1\left(f(h_{k,l}), g(h_{k,l})\right)$, $f(h_{k,l})$ and $g(h_{k,l})$ are,

$$\begin{aligned}\frac{\partial Q_1\left(f(h_{k,l}), g(h_{k,l})\right)}{\partial f(h_{k,l})} = &f(h_{k,l})[Q_2\left(f(h_{k,l}), g(h_{k,l})\right) \\ &- Q_1\left(f(h_{k,l}), g(h_{k,l})\right)]\end{aligned} \tag{20}$$

$$\begin{aligned}\frac{\partial Q_1\left(f(h_{k,l}), g(h_{k,l})\right)}{\partial g(h_{k,l})} = &g(h_{k,l})[Q_0\left(f(h_{k,l}), g(h_{k,l})\right) \\ &- Q_1\left(f(h_{k,l}), g(h_{k,l})\right)]\end{aligned} \tag{21}$$

$$\frac{\partial f(h_{k,l})}{\partial h_{k,l}} = \frac{A_{k,l}}{2\sqrt{h_{k,l}}}, \qquad \frac{\partial g(h_{k,l})}{\partial h_{k,l}} = -\frac{B_{k,l}}{2(h_{k,l})^{(3/2)}} \tag{22}$$

Hence, the derivative in (19) becomes,

$$\begin{aligned}&\frac{\partial P_{k,l}^{\text{out}}(h_{k,l})}{\partial h_{k,l}} = \\ &- \frac{A_{k,l}^2}{2}[Q_2\left(f(h_{k,l}), g(h_{k,l})\right) - Q_1\left(f(h_{k,l}), g(h_{k,l})\right)] \\ &- \frac{B_{k,l}^2}{2h_{k,l}^2}[Q_1\left(f(h_{k,l}), g(h_{k,l})\right) - Q_0\left(f(h_{k,l}), g(h_{k,l})\right)]\end{aligned} \tag{23}$$

The generalized Marcum Q-function $Q_n(a,b)$ is strictly increasing in n for all positive a and b [21]. Then, the derivative in (23) is strictly negative and therefore, the outage probability with respect to the channel gain $h_{k,l}$ is strictly decreasing. Consequently, the optimal solution $h_{k,l}^*$ of the optimization problem $(\mathbf{P'_{k,l}})$ is $H_{k,l,max}$, which can be written in terms of the link distance as follows,

$$h_{k,l}^* = H_{k,l,max} = C_{k,l}\left[d_{k,min}\right]^{\beta_{k,l}} \tag{24}$$

where $C_{k,l}$ and $\beta_{k,l}$ are given by,

$$C_{k,l} = \begin{cases} \left(d_k^0\right)^{\alpha_{AG}} 10^{-\frac{L_{AG}(d_k^0)|_{dB}+\chi}{10}} & (k,l) = \{(1,U),(2,D)\} \\ \left(\frac{c}{4\pi f}\right)^{\alpha_{GA}} & (k,l) = \{(1,D),(2,U)\} \end{cases}, \tag{25}$$

$$\beta_{k,l} = \begin{cases} -\alpha_{AG} & (k,l) = \{(1,U),(2,D)\} \\ -\alpha_{GA} & (k,l) = \{(1,D),(2,U)\} \end{cases}. \tag{26}$$

Also, $d_{k,min}$ is the minimum communication distance which can be obtained by solving the following problem,

$$(\mathbf{P^D_{k,l}}): \min_{x_k, y_k} \quad d_k\left(x_k, y_k\right) \tag{27a}$$

$$\text{s. t.} \quad x_{k,min} \leq x_k \leq x_{k,max}, \tag{27b}$$

$$y_{k,min} \leq y_k \leq y_{k,max}. \tag{27c}$$

Using the constraints on the tether length and the angle of the UAV in (15), we obtain the constraints on the (x_k, y_k), $k = 1, 2$ coordinates which have the following minimum and maximum values,

$$\begin{aligned}(x_{k,min}, y_{k,min}) &= (\eta_{k,min}\cos\theta_{k,max}, \eta_{k,min}\sin\theta_{k,min}) \\ (x_{k,max}, y_{k,max}) &= (\eta_{k,max}\cos\theta_{k,min}, \eta_{k,max}\sin\theta_{k,max})\end{aligned} \tag{28}$$

The partial derivatives of $d_k\left(x_k, y_k\right)$ are expressed as follows,

$$\begin{aligned}\frac{\partial d_k(x_k,y_k)}{\partial x_k} &= \begin{cases} \frac{x_1 - x_{\text{TBS}}}{d_1(x_1,y_1)}, & k = 1 \\ \frac{x_2 - x_{\text{AntS}}}{d_2(x_2,y_2)}, & k = 2 \end{cases}, \\ \frac{\partial d_k(x_k,y_k)}{\partial y_k} &= \begin{cases} \frac{y_1 - y_{\text{TBS}}}{d_1(x_1,y_1)}, & k = 1 \\ \frac{y_2 - y_{\text{AntS}}}{d_2(x_2,y_2)}, & k = 2 \end{cases},\end{aligned} \tag{29}$$

Since we have that $x_{1,max} \leq x_{\text{TBS}}$ and $x_{2,max} \leq x_{\text{AntS}}$, then the distance $d_k\left(x_k, y_k\right)$ is decreasing with respect to x_k. Similarly, since $y_{1,min} \geq y_{\text{TBS}}$ and $y_{2,min} \geq y_{\text{AntS}}$, the distance is increasing with respect to y_k. Hence, the minimum distance is $d_{k,min} = d_k(x_{k,max}, y_{k,min})$.

Therefore, the optimal placement of the UAVs is defined by, $(\eta_k^*, \theta_k^*) = \left(\sqrt{x_{k,max}^2 + y_{k,min}^2}, \arctan\left(\frac{y_{k,min}}{x_{k,max}}\right)\right)$.

2) Optimal UAV placement for Link 3:

For the third link, we minimize the outage probability by optimizing the position of the two tethered UAVs (sUAV and gUAV) in the 2D plane. Hence the third optimization problem $(\mathbf{P_{3,l}})$, $l = U, D$ is expressed as,

$$(\mathbf{P_{3,l}}): \min_{\eta_1,\theta_1,\eta_2,\theta_2} \quad P_{3,l}^{\text{out}}\left(\eta_1, \theta_1, \eta_2, \theta_2\right) \tag{30a}$$

$$\text{s. t.} \quad \eta_{1,min} \leq \eta_1 \leq \eta_{1,max}, \tag{30b}$$

$$\theta_{1,min} \leq \theta_1 \leq \theta_{1,max}, \tag{30c}$$

$$\eta_{2,min} \leq \eta_2 \leq \eta_{2,max}, \tag{30d}$$

$$\theta_{2,min} \leq \theta_2 \leq \theta_{2,max}. \tag{30e}$$

To solve the optimization problem $(\mathbf{P_{3,l}})$, we follow similar strategy employed in the problem resolution for the first two links. First, the solution $h_{3,l}^*$ of the corresponding simplified problem is,

$$h_{3,l}^* = C_{3,l}\left[d_{3,min}\right]^{-\alpha_{AA}}, \quad C_{3,l} = \left(\frac{c}{4\pi f}\right)^{\alpha_{AA}} \tag{31}$$

The minimum distance $d_{3,min}$ is determined by solving the following optimization problem,

$$(\mathbf{P^D_{3,l}}): \min \quad d_k\left(x_3^{\text{sUAV}}, x_3^{\text{gUAV}}, y_3^{\text{sUAV}}, y_3^{\text{gUAV}}\right) \tag{32a}$$

$$\text{s. t.} \quad x_{3,min}^{\text{sUAV}} \leq x_3^{\text{sUAV}} \leq x_{3,max}^{\text{sUAV}}, \tag{32b}$$

$$y_{3,min}^{\text{sUAV}} \leq y_3^{\text{sUAV}} \leq y_{3,max}^{\text{sUAV}}, \tag{32c}$$

$$x_{3,min}^{\text{gUAV}} \leq x_3^{\text{gUAV}} \leq x_{3,max}^{\text{gUAV}}, \tag{32d}$$

$$y_{3,min}^{\text{gUAV}} \leq y_3^{\text{gUAV}} \leq y_{3,max}^{\text{gUAV}} \tag{32e}$$

where the constraints on the two UAVs coordinates are defined by minimum and maximum values in (28), except for x coordinate of the sUAV which takes into account the ship's position where $x_3^{\text{sUAV}} \in [x_S - \eta_{1,max}\cos\theta_{1,min}, x_S - \eta_{1,min}\cos\theta_{1,max}]$.

To ensure an Air-to-Air communication between the two UAVs, we assume that both UAVs are flying at similar heights, which can be set to their maximum value to minimise the distance i.e. $y_{3,max}^{\text{sUAV}} = y_{3,max}^{\text{gUAV}}$. Then, since we have that $x_{3,min}^{\text{sUAV}} \geq x_{3,max}^{\text{gUAV}}$, the distance is increasing and deceasing with respect to x_3^{sUAV} and x_3^{gUAV}, respectively. Thus, the minimum distance is $d_{3,min} = d_3(x_{3,min}^{\text{sUAV}}, y_{3,max}^{\text{sUAV}}, x_{3,max}^{\text{gUAV}}, y_{3,max}^{\text{gUAV}})$.

Therefore, the optimal placement of the sUAV and gUAV is defined by,

$$(\eta_1^*, \theta_1^*) = \left(\sqrt{(x_{3,min}^{\text{sUAV}})^2 + (y_{3,max}^{\text{sUAV}})^2}, \arctan\left(\frac{y_{3,max}^{\text{sUAV}}}{x_{3,min}^{\text{sUAV}}}\right)\right),$$

$$(\eta_2^*, \theta_2^*) = \left(\sqrt{(x_{3,max}^{\text{gUAV}})^2 + (y_{3,max}^{\text{gUAV}})^2}, \arctan\left(\frac{y_{3,max}^{\text{gUAV}}}{x_{3,max}^{\text{gUAV}}}\right)\right).$$

IV. Numerical Results

In this section, we present our numerical results. Table I summarizes the simulation parameters. Also, the y coordinates (the heights) of the TBS and the antenna ship are $y_{\text{TBS}} = 30m$ and $y_{\text{AntS}} = 5m$. The minimum and maximum values of the tether length and angle of the sUAV and the gUAV are $\eta_{n,min} = 200m$, $\eta_{n,max} = 800m$, $\theta_{n,min} = \frac{\pi}{6}$ and $\theta_{n,max} \approx \frac{\pi}{2}$, for $n = 1, 2$. The antenna gains for the TBS, UAV, and ship are 12 dB, 10 dB and 10 dB [11], [16]. We set the minimum SNR $\gamma_{k,l}^{min}$ to 5 dB, 10 dB and 15 dB.

Parameter	Value	Parameter	Value
α_{AA}	1.9 [19]	P_{sUAV}	30 W [16]
α_{AG}	2.2 [18]	P_{AntS}	20 W
α_{GA}	2.51 [19]	P_{TBS}	40 W [16]
f	2 GHz	P_{gUAV}	30 W
$\sigma^2_{N_k}$	10^{-10} W	d_k^0	2.2 Km [18]
σ_χ	4.2 dB [18]	$L_{AG}(d_k^0)\|_{dB}$	100.7 dB [18]

TABLE I: Simulation Parameters

To investigate the coverage performance of the three links, we observe the variations of the outage probability versus the distance between the ship and the shore, presented in Fig.2 and Fig.3 in case of the downlink and the uplink, respectively for the scenarios of Link 1 (TBS−sUAV), Link 2 (Ship−gUAV) [16], and Link 3 (gUAV−sUAV). First, the results shows that the outage probability is increasing in terms of the SNR $\gamma_{k,l}^{min}$ which is expected because high SNR requirements limits the coverage performance of the links.

Second, for link 1 where the UAV is tethered to the ship at sea, we notice that the uplink is more reliable than the downlink. Meanwhile for link 2 where the UAV is installed on the shore, the downlink is more reliable than the uplink. This behaviour can be explained by the type of the wireless channel in each case. In fact, the channel of the uplink of link 1 and downlink of link 2 is an Air-to-Ground channel, having a lower path loss exponent than the Ground-to-Air channel describing the case of the downlink of the first link and uplink of second link. Therefore, taking advantage of both links, it would be beneficial to employ link 1 for the uplink and link 2 for the downlink.

Third, regarding link 3 where two UAVs are used, the uplink and downlink have similar outage probability because of the symmetric Air-to-Air communications. As illustrated in Fig.2 and Fig.3, the third link presents a better performance compared to the other links, in terms of outage probability, not only because the Air-to-Air channel has lower path loss, but also because the distance between the two UAVs, which are flying at same heights, of the third link's is shorter compared to link 1 and 2, for the same ship-shore range. Nevertheless, we note that, in terms of rate performance, using two UAVs operating in a similar fashion to link 1 and 2 (sUAV for uplink and gUAV for downlink) may be better than employing link 3 with Air-to-Air communications. In fact, the available band should be divided between the UAVs to avoid interference in the second case, while the entire band can be used for both uplink and downlink without interference, in the first case, increasing the achievable rate.

V. Conclusion

In this work, we explored the use of tethered UAVs in maritime communications. In particular, we considered three scenarios where the UAV is either installed on the shore, tethered to the ship, or both. Then, we optimized the outage probability to derive the optimal UAV placement for the uplink and downlink in each scenario. In terms of the UAV tether length and the angle it makes with the horizontal, the optimization problem is not convex, hence, we derived the optimal UAV placement by solving a simplified problem that minimizes the outage probability with respect to the channel gain. The simulation results showed that adopting two UAVs offers more reliable uplink and downlink, compared to the other scenarios.

References

[1] S. Dang, O. Amin, B. Shihada, and M. S. Alouini, "What should 6G be?" *Nature Electronics*, vol. 3, pp. 20–29, 1 2020.

[2] B. Shihada, O. Amin, C. Bainbridge, S. Jardak, O. Alkhazragi, T. K. Ng, B. Ooi, M. Berumen, and M.-S. Alouini, "Aqua-fi: Delivering internet underwater using wireless optical networks," *IEEE Commun. Mag.*, vol. 58, no. 5, pp. 84–89, 2020.

[3] S. Ammar, O. Amin, M.-S. Alouini, and B. Shihada, "Energy-aware underwater optical system with combined solar cell and SPAD receiver," *IEEE Commun. Lett.*, vol. 26, no. 1, pp. 59–63, 2021.

[4] A. Celik, N. Saeed, B. Shihada, T. Y. Al-Naffouri, and M.-S. Alouini, "A software-defined opto-acoustic network architecture for internet of underwater things," *IEEE Commun. Mag.*, vol. 58, no. 4, pp. 88–94, 2020.

[5] T. Shafique, O. Amin, M. Abdallah, I. S. Ansari, M.-S. Alouini, and K. Qaraqe, "Performance analysis of single-photon avalanche diode underwater VLC system using ARQ," *IEEE Photonics Journal*, vol. 9, no. 5, pp. 1–11, 2017.

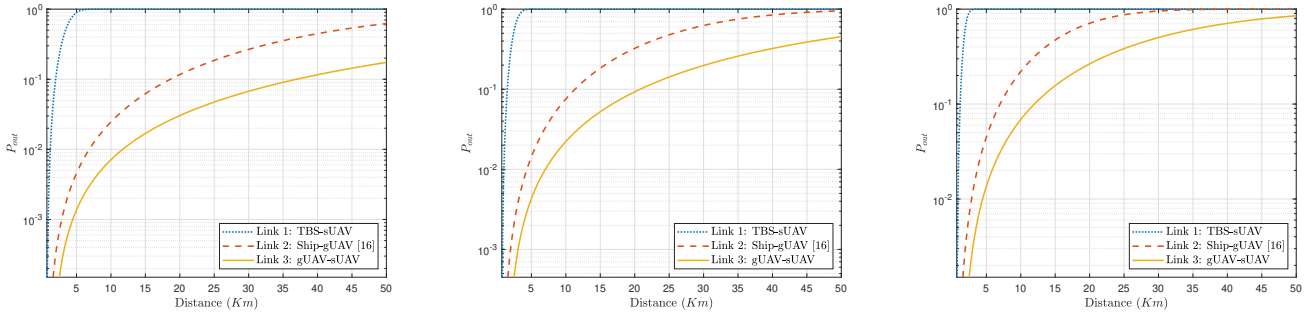

(a) SNR = 5 dB (b) SNR = 10 dB (c) SNR = 15 dB

Fig. 2: Outage probability versus the distance between ship and shore for downlink.

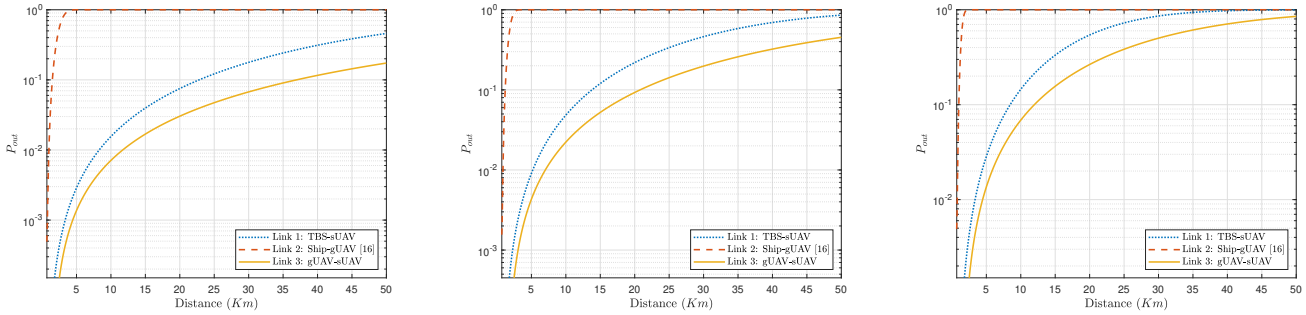

(a) SNR = 5 dB (b) SNR = 10 dB (c) SNR = 15 dB

Fig. 3: Outage probability versus the distance between ship and shore for uplink.

[6] F. S. Alqurashi, A. Trichili, N. Saeed, B. S. Ooi, and M.-S. Alouini, "Maritime communications: A survey on enabling technologies, opportunities, and challenges," *IEEE Internet Things J.*, vol. 10, no. 4, pp. 3525–3547, 2023.

[7] S.-W. Jo and W.-S. Shim, "LTE-maritime: High-speed maritime wireless communication based on LTE technology," *IEEE Access*, vol. 7, pp. 53 172–53 181, 2019.

[8] M. M. Azari, S. Solanki, S. Chatzinotas, O. Kodheli, H. Sallouha, A. Colpaert, J. F. Mendoza Montoya, S. Pollin, A. Haqiqatnejad, A. Mostaani, E. Lagunas, and B. Ottersten, "Evolution of non-terrestrial networks from 5G to 6G: A survey," *IEEE Communications Surveys & Tutorials*, vol. 24, no. 4, pp. 2633–2672, 2022.

[9] S. Ammar, C. P. Lau, and B. Shihada, "An in-depth survey on virtualization technologies in 6G integrated terrestrial and non-terrestrial networks," *arXiv preprint arXiv:2312.01895*, 2023.

[10] P. Hadinger, "Inmarsat global xpress the design, implementation, and activation of a global Ka-band network," in *33rd AIAA ICSSC*, 2015, p. 4303.

[11] X. Li, W. Feng, Y. Chen, C. X. Wang, and N. Ge, "Maritime coverage enhancement using UAVs coordinated with hybrid satellite-terrestrial networks," *IEEE Trans. Commun.*, vol. 68, pp. 2355–2369, 4 2020.

[12] S. M. Insights. Fisheries & Aquaculture. [Online]. Available: https://www.statista.com/markets/421/topic/497/fisheries-aquaculture/

[13] B. E. Y. Belmekki and M.-S. Alouini, "Unleashing the potential of networked tethered flying platforms: Prospects, challenges, and applications," *IEEE Open J. Veh. Technol.*, vol. 3, pp. 278–320, 2022.

[14] R. Campos, T. Oliveira, N. Cruz, A. Matos, and J. M. Almeida, "BLUECOM+: Cost-effective broadband communications at remote ocean areas," in *OCEANS 2016-Shanghai*, 2016, pp. 1–6.

[15] Y. Wang, X. Fang, W. Feng, Y. Chen, N. Ge, and Z. Lu, "On-demand coverage for maritime hybrid satellite-UAV-terrestrial networks," in *2020 WCSP*, 2020, pp. 483–488.

[16] X. Fang, W. Feng, Y. Wang, Y. Chen, N. Ge, Z. Ding, and H. Zhu, "NOMA-based hybrid satellite-UAV-terrestrial networks for 6g maritime coverage," *IEEE Trans. Wirel. Commun.*, vol. 22, no. 1, pp. 138–152, 2022.

[17] J. Wang, H. Zhou, Y. Li, Q. Sun, Y. Wu, S. Jin, T. Q. Quek, and C. Xu, "Wireless channel models for maritime communications," *IEEE Access*, vol. 6, pp. 68 070–68 087, 2018.

[18] D. W. Matolak and R. Sun, "Air–ground channel characterization for unmanned aircraft systems—part I: Methods, measurements, and models for over-water settings," *IEEE Trans. Veh. Technol.*, vol. 66, no. 1, pp. 26–44, 2016.

[19] A. A. Khuwaja, Y. Chen, N. Zhao, M.-S. Alouini, and P. Dobbins, "A survey of channel modeling for UAV communications," *IEEE Commun. Surv. Tutor.*, vol. 20, no. 4, pp. 2804–2821, 2018.

[20] N. Goddemeier and C. Wietfeld, "Investigation of air-to-air channel characteristics and a UAV specific extension to the rice model," in *IEEE GC Wkshps*, 2015, pp. 1–5.

[21] Y. Sun, Á. Baricz, and S. Zhou, "On the monotonicity, log-concavity, and tight bounds of the generalized marcum and nuttall Q-functions," *IEEE Trans. Inf. Theory*, vol. 56, no. 3, pp. 1166–1186, 2010.